

# Long-term nitrogen fertilization alters microbial respiration sensitivity to temperature and moisture, potentially enhancing soil carbon retention in a boreal Scots pine forest

Boris Ľupek<sup>1</sup>, Aleksi Lehtonen<sup>1</sup>, Stefano Manzoni<sup>2</sup>, Elisa Bruni<sup>3</sup>, Petr Baldrian<sup>4</sup>, Etienne Richy<sup>4</sup>, Bartosz Adamczyk<sup>1</sup>, Bertrand Guenet<sup>3</sup>, and Raisa Mäkipää<sup>1</sup>

<sup>1</sup>Natural Resources Institute Finland (LUKE), Helsinki, 00790, Finland

<sup>2</sup>Department of Physical Geography and Bolin Centre for Climate Research, Stockholm University, Stockholm, 10691, Sweden.

<sup>3</sup>Laboratoire de Géologie, École Normale Supérieure (ENS), Paris, 75005, France

<sup>4</sup>Laboratory of Environmental Microbiology, Institute of Microbiology of the Czech Academy of Sciences, Prague, 14200, Czech Republic

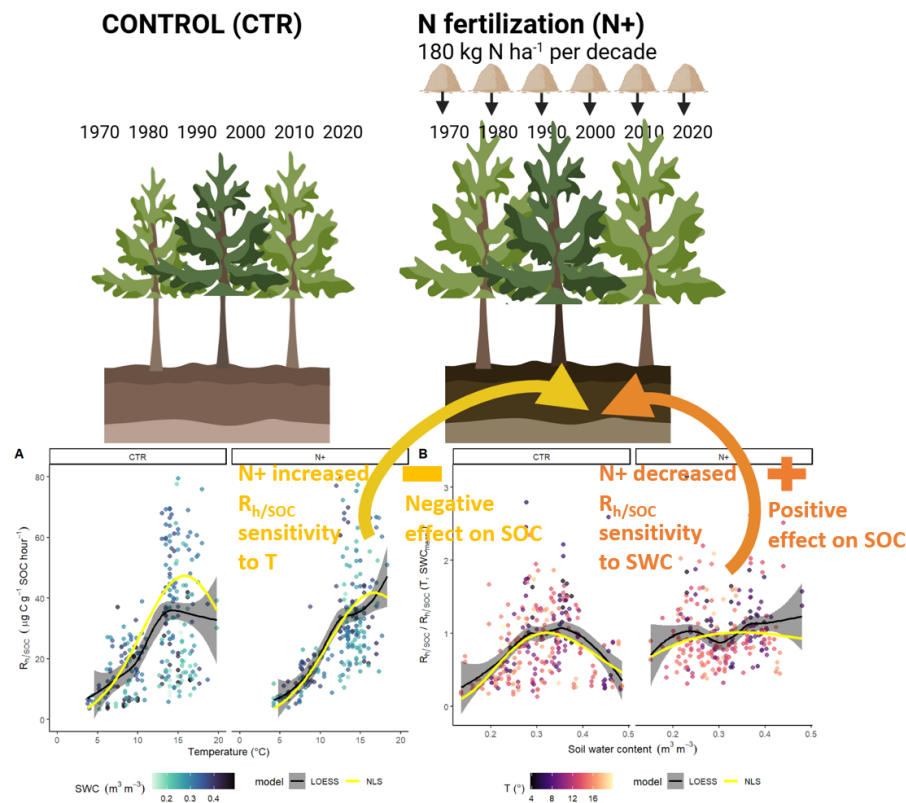
Correspondence to: Boris Ľupek (boris.tupek@luke.fi)

**Abstract.** Nutrient availability affects microbial respiration kinetics and their sensitivities to environmental conditions, thus the soil organic carbon (SOC) stocks. We examined long-term nitrogen (N) addition effects on soil heterotrophic respiration ( $R_h$ ), methane ( $CH_4$ ) oxidation, and nitrous oxide ( $N_2O$ ) emissions in an N-limited boreal Scots pine (*Pinus sylvestris*) forest, in central Finland. Measurements included long-term tree biomass monitoring (1960–2020), soil organic carbon (SOC) in 2023, monthly aboveground litterfall (2021–2023), biweekly  $CO_2$ ,  $CH_4$ , and  $N_2O$  fluxes during the 2021–2023 growing seasons, and quarter-hourly recordings of soil temperature (T) and soil water content (SWC) in both control and N-fertilized plots. Measurements included long-term 1960–2020 tree biomass monitoring, 2023 SOC, 2021–2023 monthly aboveground litterfall, 2021–2023 growing seasons biweekly  $CO_2$ ,  $CH_4$ , and  $N_2O$  fluxes, and quarter-hourly soil temperature (T), and soil water content (SWC) in both control and N-fertilized plots. We assessed mean greenhouse gas (GHG) flux differences and  $R_h$  dependence on T and SWC using polynomial and parametric non-linear regression models.

Tree biomass, litterfall and SOC increased with long-term N fertilization. However, N fertilization also significantly increased mean  $R_h$ , reduced  $CH_4$  oxidation slightly, and modestly raised  $N_2O$  emissions. SOC-normalized  $R_h$  ( $R_{h/SOC}$ ) did not significantly differ between treatments, yet relationships between  $R_{h/SOC}$  and T and SWC diverged with fertilization. In control plots,  $R_{h/SOC}$  peaked at 15.8 °C and at 16.8 °C in N-fertilized plots. Under N fertilization,  $R_{h/SOC}$  was weakly SWC-dependent, contrasting with a distinct humped SWC response in control plots, enhancing annual  $R_{h/SOC}$  in control plots. Annually, N-fertilized plots respired 10.3% of SOC ( $\pm 0.3$  standard error (SE)), compared to 12.2% ( $\pm 0.5$  SE) in controls, suggesting N fertilization promoted SOC retention. Consequently, N fertilization reduced average annual net  $CO_2$  emissions by 345.4 ( $\pm 73.6$  SE)  $-g CO_2 m^{-2} year^{-1}$ , while combined effects on  $CH_4$  and  $N_2O$  fluxes and the production energy of N fertilizer contributed annually a minor  $CO_2$ -equivalent increase of 17.7 ( $\pm 0.5$  SE)  $g CO_2-eq m^{-2} year^{-1}$ .

In conclusion, long-term N fertilization in boreal forests could reduce global warming potential of soil GHG emissions, mainly by slowing  $R_{hSOC}$ , and altering its responses to T and SWC, thereby enhancing SOC sequestration in addition to the increased tree biomass carbon sink.

Graphical abstract.



1 Introduction

40 Vegetation growth in boreal forests is primarily constrained by temperature (Jarvis and Linder, 2000) and soil nutrient availability, particularly nitrogen (N) (Näsholm et al., 1998; Höglberg et al., 2017). Atmospheric N deposition or fertilization can enhance tree biomass growth (Lupi et al., 2013; Saarsalmi and Mälikönen, 2001; Sponseller et al., 2016) and increase soil carbon (C) sequestration by promoting productivity and litter inputs while reducing decomposition rates (Janssens et al., 2010; Marshall et al., 2021; Smolander et al., 1994). This increased C storage in both tree biomass and soil after N

45 fertilization could be seen as a positive feedback effect on ecosystem C balance in Northern forests (Hyvönen et al., 2008; Mäkipää et al., 2023). However, the effects of N fertilization on organic matter (OM) decomposition and the net balance of greenhouse gas (GHG) emissions (CO<sub>2</sub>, CH<sub>4</sub>, N<sub>2</sub>O) are less well understood and equally critical for assessing the forest C balance and its global warming potential. N fertilization may reduce soil CO<sub>2</sub> emissions (Janssens et al., 2010) due to enhanced microbial carbon use efficiency (CUE) (Manzoni et al., 2012b, 2017) and decreased need for N mining from

50 ~~organic mineralization~~ organic matter (Craine et al., 2007). It may also increase N<sub>2</sub>O emissions due to greater soil N availability (Högberg et al., 2017; Öquist et al., 2024) and potentially alter CH<sub>4</sub> uptake by either increasing N availability for CH<sub>4</sub> oxidizing microbes or by competing with NH<sub>4</sub> for reduction (Öquist et al., 2024). ~~Because these soil processes could alter the forest C balance,~~ offset the enhanced tree C sink, potentially converting the ecosystem into a net C source. Evaluating the feedback of N fertilization on forest climate mitigation potential ~~thus~~ requires consideration of impacts on both tree growth

55 and OM decomposition. Moreover, full accounting of GHG emissions should include emissions associated with N fertilizer production (Osorio-Tejada et al., 2022).

The soil C balance in boreal forests, which is a dynamic balance between C input from litterfall and CO<sub>2</sub> emissions from OM decomposition, is influenced by temperature (T), soil water content (SWC), nutrient status, and vegetation composition (Deluca and Boisvenue, 2012)—all factors sensitive to forest management (Mäkipää et al., 2023; Mayer et al., 2020). For

60 example, N fertilization enhances soil N availability, promoting plant growth and litterfall (C input) while potentially reducing OM decomposition due to increased CUE ~~of N-limited~~ microbial decomposers (Manzoni et al., 2017). These effects, alongside T and SWC controls, can be integrated into soil C models (Zhang et al., 2018). ~~Consequently~~ Moreover, changes in ~~SOC decomposition dynamics related to~~ microbial community structure (e.g., activity, CUE, and biodiversity; Khurana et al., 2023) induced by fertilization can affect decomposition dynamics and may influence soil microbial respiration

65 dependencies on T and SWC. ~~For example, S~~ shifts in respiration responses to temperature due to N fertilization may attenuate CO<sub>2</sub> emissions under warming scenarios (Chen et al., 2024; Wei et al., 2017). Although the effects of N addition on moisture dependency remain understudied, interactions between T and SWC are critical for forecasting respiration responses (Pallandt et al., 2022; Sierra et al., 2017, 2015).

Empirically derived relationships between soil respiration and T and SWC are widely used in soil C models to adjust

70 decomposition rate constants (Luo et al., 2016), yet differences in SWC responses (Sierra et al., 2015) contribute to projection uncertainties (Falloon et al., 2011). Boreal forest soils with higher nutrient levels and water availability often have underestimated SOC stocks in model projections (Dalsgaard et al., 2016; Tupek et al., 2016). Moreover, SWC response curves vary with soil properties like porosity, clay content, and OM fraction (Moyano et al., 2013, 2012) and may also be influenced by soil N status. ~~Improving SOC projections would therefore require accounting for these variations.~~ Given the

75 significant spatial variability in SOC within forest sites (Muukkonen et al., 2009) and the measurement uncertainty over time (Ortiz et al., 2013), assessing changes in the T and SWC dependencies of soil CO<sub>2</sub> emissions after long-term N fertilization and applying them over multiple years could clarify the SOC sink/source dynamics.

In southern boreal region's Scots pine forests on well-drained, often N-poor mineral soils, soil CO<sub>2</sub> emissions range from 1 to 3 kg CO<sub>2</sub> m<sup>-2</sup> year<sup>-1</sup>, accounting for 70–91% of total ecosystem respiration (Tupek et al., 2008; Uri et al., 2022) and its global warming potential (GWP). Although CH<sub>4</sub> and N<sub>2</sub>O have higher GWP than CO<sub>2</sub> (27 and 273 times over a 100-year horizon, respectively; IPCC (2023)), the soil generally acts as a small CH<sub>4</sub> ~~exchange is generally a small~~ sink, and N<sub>2</sub>O emissions are negligible in these N-limited soils (Machacova et al., 2016; Matson et al., 2009; Pihlatie et al., 2007; Siljanen et al., 2020; Tupek et al., 2015).

In this study, we investigated the effects of long-term N fertilization on soil CO<sub>2</sub>, CH<sub>4</sub>, and N<sub>2</sub>O fluxes and SOC stocks in a boreal Scots pine forest. We hypothesized that (i) increased soil nitrogen availability would enhance soil organic carbon (SOC) accumulation and heterotrophic respiration (R<sub>h</sub>) due to greater biomass growth and litter inputs, while SOC-normalized R<sub>h</sub> (R<sub>h</sub>/SOC) would decline due to reduced microbial nitrogen demandmining; and (ii) nitrogen fertilization would alter CH<sub>4</sub> oxidation and increase N<sub>2</sub>O emissions compared to N-limited soils, reflecting shifts in microbial activity and substrate availability.

## 2 Methods

### 2.1 Study site and N fertilization

The Karstula forest study site is in central Finland (62°54'43.343"N, 24°34'16.021"E) (Fig. 1) and is dominated by *Pinus sylvestris* (Scots pine) with an understory comprising *Vaccinium myrtillus*, *V. vitis-idaea*, *Empetrum nigrum*, *Calluna vulgaris*, and various boreal mosses and lichens. Established on a low-fertility sandy podzol, the site corresponds to the Calluna (CT) and *Vaccinium vitis-idaea* (VT) types in the Finnish classification system (Cajander, 1949). Nitrogen (N) fertilization has been applied here since 1960, with 180 kg N ha<sup>-1</sup> potassium nitrate applied every decade until 2020.

The stand underwent thinning in 1990 and 2015. To maintain comparable management across fertilization treatments, both CTR and N-fertilized (N+) plots were thinned in 1990 with similar intensity (~20%), and again in 2015 with nearly identical intensity, reducing basal area by 36.7% (CTR) and 40.1% (N+), following the Finnish silvicultural guidelines (Tapio, www.tapio.fi), (reducing 16.2% and 26.5% of basal area (BA) for CTR and N+, respectively), and 2015 (reducing 36.7 % and 40.1% of BA for CTR and N+, respectively).

Formatted: Font: Not Italic

Formatted: Font: Not Italic

Formatted: Font: Not Italic

Formatted: Font: Not Italic

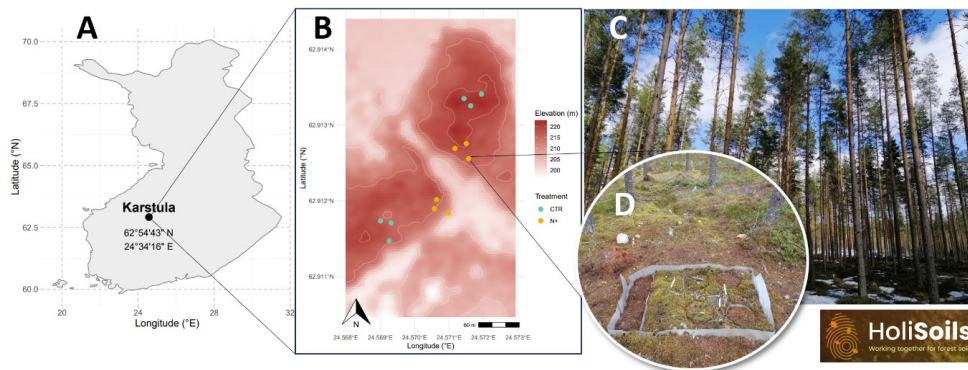


**Figure 1: Geographical location of the Karstula forest study site in Finland (A); topographical variation of the study site and the location of treatment (control CTR and N-fertilized N+) plots (B); photograph of the forest stand (C); and one of six 2 x 1 m forest floor plot groups, each with four subplots used for measuring soil greenhouse gases, soil organic C, and soil temperature and moisture following the installation of a root-exclusion fabric (D).**

## 2.2 Field measurements

### 2.2.1 Tree inventory and litterfall

Measurements of tree diameter (at 1.3 m height), total height, and crown base height have been conducted at 10-year intervals from 1960 to 2010 and every 5 years thereafter. The breast-height diameter (d1.3) of all trees has been measured using a caliper ( $\pm 1$  mm precision) once per decade since 1960, as well as after the 2015 thinning. Additionally, in a permanent subset of trees representing various size categories, tree height and crown base height have been recorded using a hypsometer (precision  $\sim 0.5$ –1 m). Mortality and thinning-related removals were recorded, and tree biomass was calculated using biomass expansion models (Repola, 2009). Litterfall rates were estimated using compartment-specific turnover rates (Lehtonen et al., 2016). From May 2021 to October 2023, litter (needles, twigs, cones) was collected monthly during the growing season using 0.8 m mesh collectors and subsequently sorted and weighed.

### 2.2.2 Soil organic carbon stock (SOC)

Soil sampling was performed in June 2023 in control and N-fertilized plots ( $n=6$  each) using a 58 mm diameter corer. Samples were stratified by layer, separating humus from mineral soil, which was sampled in 10 cm increments to a depth of 30 cm. Samples from each layer were composited across two subsites with differing rock content. Samples were dried, weighed, and sieved, and C and N contents were analyzed using dry combustion (LECO TruMac CN, LECO Corporation,

St. Joseph, MI, USA). Stoniness was assessed in the field using rod penetration (Eriksson and Holmgren, 1996) and  
125 corrected for rock fragment content following Poeplau et al. (2017).

**2.2.2 Soil greenhouse gas (GHG) fluxes, temperature, and moisture**

Soil GHG fluxes (CO<sub>2</sub>, CH<sub>4</sub>, and N<sub>2</sub>O) were measured biweekly during the growing seasons of 2021-2023 (spanning from  
20<sup>th</sup> May to 16<sup>th</sup> August in 2021, 5<sup>th</sup> May to 3<sup>rd</sup> November in 2022, and 10<sup>th</sup> May to 10<sup>th</sup> October in 2023). ~~Measurements  
were taken from 12 plots (6 plots or 3 pairs per treatment). In May 2021, three 1 × 2 m trenched areas were established per  
treatment. Each trench was lined with water-permeable geotextile to prevent root ingrowth, thereby isolating heterotrophic  
respiration (R<sub>h</sub>) from autotrophic sources (Tupek et al., 2019). Measurements were taken from 12 plots (six per treatment;  
Fig. 1b). Two plot pairs (2 × 706 cm<sup>2</sup>) were used to account for local heterogeneity in soil and microtopography at the trench  
level within of each trenched area (1 m<sup>2</sup>), while three trenched areas per treatment were used to capture spatial heterogeneity  
of each treatment at the site level (Fig. 1d). Plots in each pair were located 30 cm apart (Fig. 1c) and CTR and N<sub>±</sub> pairs were  
on average 122 m apart (Fig. 1b). As the single plot area was relatively large (706 cm<sup>2</sup>), we considered 2 plots pair to be  
representative of the trenched area (Fig. 1c) and 3 pairs to be representative of the spatial variation of the treatment. In May  
2021, each plot was trenched (1 × 2 m) and fitted with water-permeable geotextile to prevent root ingrowth, isolating  
heterotrophic respiration (R<sub>h</sub>) from autotrophic sources (Tupek et al., 2019).~~

140 Gas fluxes were measured using a non-transparent 21.7 L dynamic chamber (30 cm in diameter and height) equipped with a  
fan and connected to a LI-COR LI-7810 CH<sub>4</sub>/CO<sub>2</sub>/H<sub>2</sub>O or LI-7820 N<sub>2</sub>O/H<sub>2</sub>O trace gas analyzer (LICOR, Lincoln, NE,  
USA). Gas concentrations were recorded every second for 3 minutes, and linearity was monitored visually during the  
measurements to accept only fluxes with increasing trends in CO<sub>2</sub> concentration evolution. Fluxes were calculated from the  
stable portion of the data (Zhao, 2019). R<sub>h</sub> values (g CO<sub>2</sub> m<sup>-2</sup> h<sup>-1</sup>) were normalized to SOC content and expressed as a C  
145 fraction of SOC per hour (μg C g<sup>-1</sup> SOC h<sup>-1</sup>). The CH<sub>4</sub> and N<sub>2</sub>O concentrations were also measured during 3 min intervals  
with 5 second averaging at the 0.25 ppb precision for CH<sub>4</sub> and 0.20 ppb precision for N<sub>2</sub>O. The minimum detectable flux of  
measurements estimated using the formula by Parkin et al., (2012) was 0.0238 μg m<sup>-2</sup> h<sup>-1</sup> for CH<sub>4</sub> and 0.0524 μg m<sup>-2</sup> h<sup>-1</sup> for  
N<sub>2</sub>O.

150 ~~Continuous monitoring of s~~Soil temperature (T) and volumetric soil moisture (SWC) at 5 cm depth ~~were continuously  
monitored as achieved~~ with Soil Scout Oy sensors, recording data at 15 min intervals since June 2021. T and SWC were  
matched with flux data by timestamp.

**2.3 Data analysis**

All data analyses and visualizations were conducted using R software (R Core Team, 2023). [The full data set and the R code](#)  
155 [for producing the analysis and results described below are available on Zenodo \(Tupek et al. 2024, Tupek B., 2024\).](#) A one-

way ANOVA was employed to test the effect of N fertilization on greenhouse gas (GHG) fluxes. Since the data were collected at relatively low temporal frequency (biweekly), the degree of temporal autocorrelation was substantially lower than in high-frequency (e.g., hourly) automated measurements. Therefore, no additional correction for autocorrelation was applied. The independence assumption of ANOVA was considered reasonably met under these conditions.

Two regression approaches were used to characterize the dependency of  $R_{h/SOC}$  on T and SWC: (i) local polynomial regression (LOESS) to assess the functional form of  $R_{h/SOC}$  dependencies on combined T and SWC ( $R_{h/SOC}(T, SWC)$ ) separately for the N-fertilized (N+) and control (CTR) plots; and (ii) nonlinear least squares (NLS) regression, guided by LOESS to identify suitable mathematical forms. The LOESS and NLS models for  $R_{h/SOC}$  dependency on SWC alone were compared using  $R_{h/SOC}$  ratios normalized by  $R_{h/SOC}(T, SWC_{mean})$ .

In approach (ii), the combined T and SWC dependency of  $R_{h/SOC}$  was modeled by multiplying a Gaussian T function as described in Tuomi et al. (2008) with a Ricker function for SWC (Bolker, 2008) (Eq. 1):

$$R_{h/SOC}(T, SWC) = e^{(\beta_1 T + \beta_2 T^2)} (a SWC e^{(-b SWC)})^c, \quad (1)$$

where  $\beta_1$  and  $\beta_2$  are parameters controlling the exponential T response, ~~and~~ parameters a determines the initial slope and rescales the whole function, exponent b describes the post-optimal decline, and exponent c modulates the sharpness of the peak height of the SWC response.

Model performance was assessed using proportion of explained variance ( $R^2$ ), root mean square error (RMSE), mean bias error (MBE), and mean absolute error (MAE) derived from model residuals. Model robustness was further evaluated with 10-fold cross-validation (Kuhn, 2008).

Once the parameters of the T and SWC response were determined, the NLS regression was used to extrapolate  $R_{h/SOC}$  to continuous hourly data and to upscale  $R_{h/SOC}$  to the annual level.

Annual  $CH_4$  and  $N_2O$  fluxes were estimated by scaling the treatment-specific mean hourly flux values without considering T and SWC effects. The global warming potential (GWP) was calculated using the AR6 GWP-100 values (27 for  $CH_4$  and 273 for  $N_2O$ ) (IPCC, 2023). As flux data were unavailable for the November–March period, the  $CH_4$  and  $N_2O$  annual estimates are limited to the extrapolating the conditions of Apr–Oct, during which fluxes are generally higher.

The ~~asseeiated~~ emissions associated with fertilizers production were accounted for according to Osorio-Tejada et al. (2022). We estimated the  $CO_2$  emissions associated with six nitrogen fertilization events, which occurred once per decade between 1960 and 2020. The applied nitrogen fertilization rate was  $180 \text{ kg N ha}^{-1}$  per event. Converting this to ammonia ( $NH_3$ ) using the molecular weight ratio of  $NH_3$  to N (17.031/14.007) resulted in an estimated  $218.86 \text{ kg NH}_3 \text{ ha}^{-1}$  per fertilization event.



Given an emission factor of 2.96 kg CO<sub>2</sub> per kg NH<sub>3</sub>, this corresponds to 647.93 kg CO<sub>2</sub> ha<sup>-1</sup> per event. Over six fertilization events spanning 60 years, the annualized CO<sub>2</sub> emission was calculated as 64.79 kg CO<sub>2</sub> ha<sup>-1</sup> yr<sup>-1</sup>, equivalent to approximately 6.5 g CO<sub>2</sub> m<sup>-2</sup> yr<sup>-1</sup>.

### 3 Results

#### 3.1 N fertilization enhanced tree biomass, litterfall, and SOC

N fertilization led to increased tree stand biomass and litterfall in N+ compared to CTR plots, ~~based on tree inventory and biomass and litter models~~. Despite reductions following thinning events, tree biomass was highest in 2014 for both treatments (9 kg C m<sup>-2</sup> in N+ and 7 kg C m<sup>-2</sup> in CTR), decreasing to 6 and 5 kg C m<sup>-2</sup>, respectively, by 2020 due to thinning in 2015 (Fig. 2a). This thinning led to peak litter input in 2015 (1.5 kg C m<sup>-2</sup> in N+ and 1 kg C m<sup>-2</sup> in CTR), which then stabilized around 0.6 and 0.5 kg C m<sup>-2</sup> due to ~~the presence of~~ fewer trees (Fig. 2a). Litter fraction accounted for 16% of N+ and 14% of CTR biomass in 2015, falling to 10% for both by 2020. Monthly litterfall, including needles, branches, and cones, was significantly higher in N+ (25.1 g m<sup>-2</sup> month<sup>-1</sup>) than in CTR (14.3 g m<sup>-2</sup> month<sup>-1</sup>) plots from 2021 to 2023 (Fig. 2b). SOC tended to be higher under N fertilization, from 4.9 kg C m<sup>-2</sup> in CTR to 5.6 kg C m<sup>-2</sup> in N+, but the difference was not statistically significant. SOC also increased under N fertilization, from 4.9 kg C m<sup>-2</sup> in CTR to 5.6 kg C m<sup>-2</sup> in N+ (Fig. 2c).

205

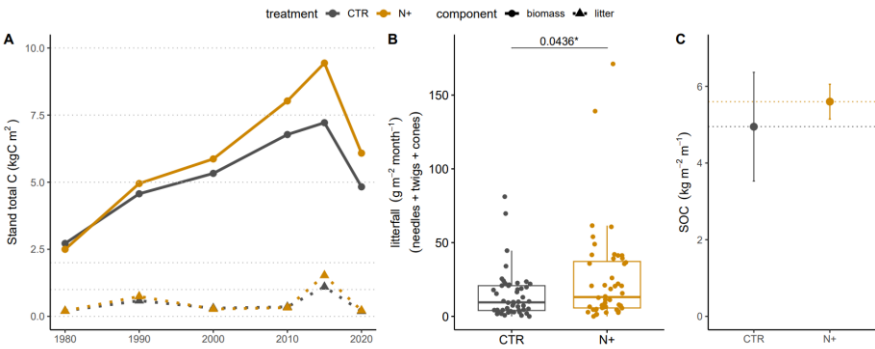


Figure 2: Biomass, litterfall, and SOC in control (CTR) and N-fertilized (N<sup>+</sup>) stands. (A) Estimated tree biomass and litterfall from 1980 to 2020 forest tree stands inventory measurements. (B) Monthly litterfall from July 2021 to October 2023 (box plot shows median, quartiles, and outliers). (C) SOC ~~stock over~~ 1 m depth in 2023 (error bars indicate minimum and maximum values across replicates).

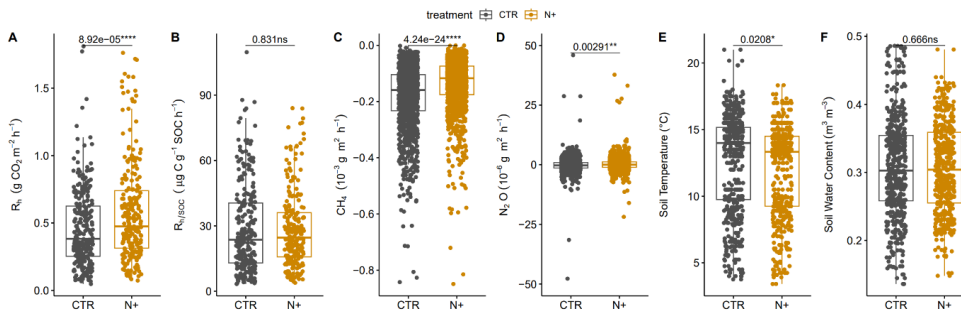
210

3.2 N fertilization effects **on** mean CO<sub>2</sub>, CH<sub>4</sub>, and N<sub>2</sub>O fluxes but not **on** SOC-normalized CO<sub>2</sub>

Pairwise ANOVA showed that mean annual soil microbial **respiration**  $R_h$  (g CO<sub>2</sub> m<sup>-2</sup> h<sup>-1</sup>) was significantly higher in N+ (0.58 ± 0.01 **standard error**, SE) than in CTR plots (0.46 ± 0.01 SE) (F-value 15.96, degrees of freedom 449, p-value 8.92e-05) (Fig. 3a). However,  $R_h$  normalized by SOC (μg C g<sup>-1</sup> SOC h<sup>-1</sup>) did not differ significantly between N+ (28.3 ± 1.1 SE) and CTR plots (28.6 ± 1.1 SE) (Fig. 3b).

CH<sub>4</sub> oxidation was slower in N+ (-0.14 ± 0.002 SE mg CH<sub>4</sub> m<sup>-2</sup> h<sup>-1</sup>) than in CTR (-0.18 ± 0.002 SE mg CH<sub>4</sub> m<sup>-2</sup> h<sup>-1</sup>) (Fig. 3c), with annual CH<sub>4</sub> oxidation rates of -1.58 g CH<sub>4</sub> m<sup>-2</sup> y<sup>-1</sup> in CTR and -1.21 g CH<sub>4</sub> m<sup>-2</sup> y<sup>-1</sup> in N+ plots. Mean net N<sub>2</sub>O exchange was significantly lower than zero in CTR (-0.25 ± 0.09 SE μg N<sub>2</sub>O m<sup>-2</sup> h<sup>-1</sup>), while in N+ it was positive (0.22 ± 0.06 SE μg N<sub>2</sub>O m<sup>-2</sup> h<sup>-1</sup>), resulting in a mean annual difference of 4.17 mg N<sub>2</sub>O m<sup>-2</sup> y<sup>-1</sup> between treatments (Fig. 3d). The method detection limits were smaller than SE of mean CH<sub>4</sub> and N<sub>2</sub>O fluxes.

Average T at 5 cm depth was higher in CTR (12.6 ± 0.17 SE °C) than in N+ (12.0 ± 0.16 SE °C) (Fig. 3e), while SWC at 5 cm depth (0.31 m<sup>3</sup> m<sup>-3</sup>) did not differ significantly between treatments (Fig. 3f). Mean annual T was 5.92 ± 0.18 SE °C in CTR and 5.83 ± 0.17 SE °C in N+, with an annual SWC of 0.31 ± 0.002 SE m<sup>3</sup> m<sup>-3</sup> for both (Fig. S1). Soil T increased rapidly after snowmelt in April, with cooler summer conditions in 2022 than in 2021 and 2023. SWC ranged from 0.07 to 0.42 m<sup>3</sup> m<sup>-3</sup>, dropping below 0.2 m<sup>3</sup> m<sup>-3</sup> during drought conditions in summer 2021 (Fig. S1, S2).  $R_h$  showed sensitivity to T and SWC, rising with warmer conditions and declining in dry periods, then recovering after rewetting events (Fig. S2). However, this pattern was more pronounced in CTR than in N+ plots. Part of the variation in soil moisture between CTR and N+ plots (located on average 122 m apart) could be attributed to the measured topsoil humus layer being affected by microscale variations of vertical and lateral water flows due to **variable** microtopography (Fig. 1b).



Formatted: Subscript

Figure 3: Soil (A) heterotrophic respiration ( $R_h$ ,  $\text{g CO}_2 \text{ m}^{-2} \text{ h}^{-1}$ ), (B)  $R_h$  normalized by SOC ( $\mu\text{g C g}^{-1} \text{ SOC h}^{-1}$ ), (C) net  $\text{CH}_4$  flux ( $\text{mg CH}_4 \text{ m}^{-2} \text{ h}^{-1}$ ), (D) net  $\text{N}_2\text{O}$  flux ( $\mu\text{g N}_2\text{O m}^{-2} \text{ h}^{-1}$ ), (E) soil temperature ( $T$ ,  $^{\circ}\text{C}$ ), and (F) soil volumetric water content (SWC,  $\text{m}^3 \text{ m}^{-3}$ ) for  $\text{N}^+$  and CTR plots in 2021, 2022, and 2023 field campaigns.

Formatted: Subscript

Formatted: Subscript

### 3.3 N fertilization altered $R_{h/\text{SOC}}$ dependencies on $T$ and SWC

LOESS and NLS regression models showed similar  $R_{h/\text{SOC}}$  dependencies on  $T$  and SWC (Fig. 4a, 4b). In CTR and  $\text{N}^+$ , NLS models indicated a  $T$  optimum at  $15.8^{\circ}\text{C}$  and  $16.8^{\circ}\text{C}$ , respectively, above which decomposition was limited by dry soil conditions. Thus  $R_{h/\text{SOC}}$  in CTR at  $T$  below the optimum rose more steeply compared to  $\text{N}^+$  plots (Fig. 4a).

The  $R_{h/\text{SOC}}$  revealed an SWC optimum in CTR, while in  $\text{N}^+$  plots the  $R_{h/\text{SOC}}$  - SWC dependency was less pronounced (Fig. 4b). The  $R_{h/\text{SOC}}$  was maximized at  $\text{SWC} = 0.32 \text{ m}^3 \text{ m}^{-3}$  in CTR and at  $\text{SWC} = 0.35 \text{ m}^3 \text{ m}^{-3}$  in  $\text{N}^+$ , and in CTR it declined more steeply under both drier and wetter conditions than in  $\text{N}^+$ .

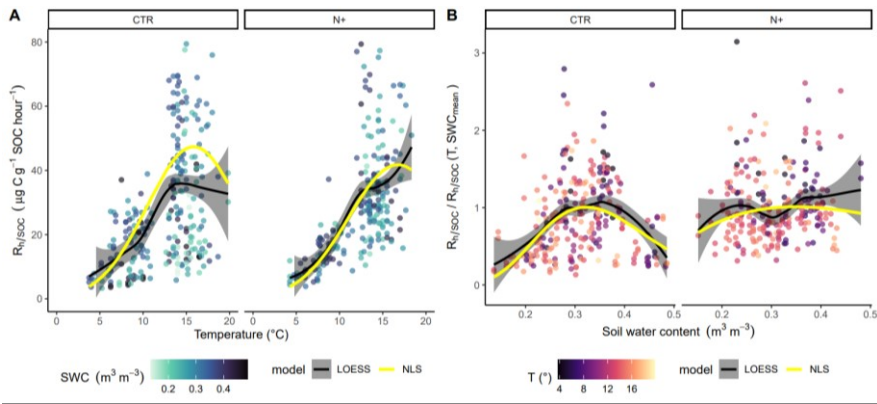


Figure 4: (A) Dependence of soil microbial respiration normalized by soil organic carbon ( $R_{h/\text{SOC}}$ ,  $\mu\text{g C g}^{-1} \text{ SOC h}^{-1}$ ) on soil temperature at 5 cm depth ( $T$ ,  $^{\circ}\text{C}$ ). (B) Ratio of measured  $R_{h/\text{SOC}}$  to modeled  $R_{h/\text{SOC}}(T, \text{SWC}_{\text{mean}})$  as a function of volumetric water content (SWC,  $\text{m}^3 \text{ m}^{-3}$ ) at 5 cm depth. Panels display results separately for control (CTR) and N-fertilized ( $\text{N}^+$ ) plots. Shading of turquoise points in (A) reflects varying SWC, while shading of red points in (B) corresponds to variation in  $T$ . Black lines indicate local polynomial regression (LOESS) fits with gray ribbons showing 95% confidence intervals; yellow lines represent nonlinear least square (NLS) regression model fits. The NLS lines in (A) are modeled as  $R_{h/\text{SOC}}(T, \text{SWC}_{\text{mean}})$  and in (B) as  $R_{h/\text{SOC}}(T, \text{SWC})/R_{h/\text{SOC}}(T, \text{SWC}_{\text{mean}})$ .

Model parameters and fit statistics for the NLS regression model are provided in Table 1 and Table 2. In CTR, the Ricker power parameter  $c$  significantly differed from one, indicating suppressed respiration in non-optimal SWC conditions. The model parameters describing functional dependencies on soil moisture were statistically ~~significant~~ different from zero for CTR but not for N+ (Table 1). While not statistically ~~significant~~ different from zero in N+ plots, the  $c$  value near 1 suggests a relatively flat response of  $R_{hSOC}$  to SWC. In contrast, a ~~significant~~ high  $c$  value ( $\approx 8$ ,  $p < 0.001$ ) in CTR plots indicates a peaked moisture response, supporting a stronger ~~the role of~~ effect of moisture limitation on decomposition under ambient conditions (Table 1). However, Neither the CTR nor N+ models showed bias (Table 2 and S1). NLS model fit metrics showed that  $R^2$ , RMSE, MBE, and MAE values were comparable between CTR and N+ models (Table 2). RMSE and MAE for NLS models fell within the range of standard deviations from 10-fold cross-validation (Table S1). The model accuracy was generally higher in N+ than in CTR plots (Table 2).

270 Table 1: Parameter estimates with standard errors (SE) and p-values for combined temperature and SWC models (Eq. 1:  $\beta_1$ ,  $\beta_2$ , a, b, and c).

Treatment	Parameter	Estimate	Std. ErrorSE	p-value
CTR	$\beta_1$	0.545	0.101	<0.001
	$\beta_2$	-0.017	0.004	<0.001
	a	7.967	0.703	<0.001
	b	3.101	0.073	<0.001
	c	8.045	1.347	<0.001
N+	$\beta_1$	0.515	0.105	<0.001
	$\beta_2$	-0.015	0.004	<0.001
	a	5.317	3.250	0.103
	b	2.871	0.432	<0.001
	c	1.500	1.063	0.160

275 Table 2: Goodness-of-fit statistics for NLS models based on combined temperature and moisture (Eq. 1): proportion of explained variance ( $R^2$ ), root mean square error (RMSE), mean bias error (MBE), and mean absolute error (MAE). RMSE, MBE and MAE in  $\mu\text{g C g}^{-1} \text{SOC h}^{-1}$ .

Treatment	$R^2$	RMSE	MBE	MAE
$\mu\text{g C g}^{-1} \text{SOC h}^{-1}$				
CTR	0.41	15.55	-0.33	11.42
N+	0.40	13.36	-0.48	9.28

3.4 N addition moderates the impact of soil moisture on modeled respiration

280 The model accuracy was generally higher in N+ than in CTR plots (Table 2). However, the soil moisture effects on  $R_{\text{SOC}}(T, \text{SWC})$  were more pronounced in CTR and N+ plots, as evidenced by larger decline and increase of respiration rates during year 2021 with severe drought (Fig. 5a).

Formatted Table

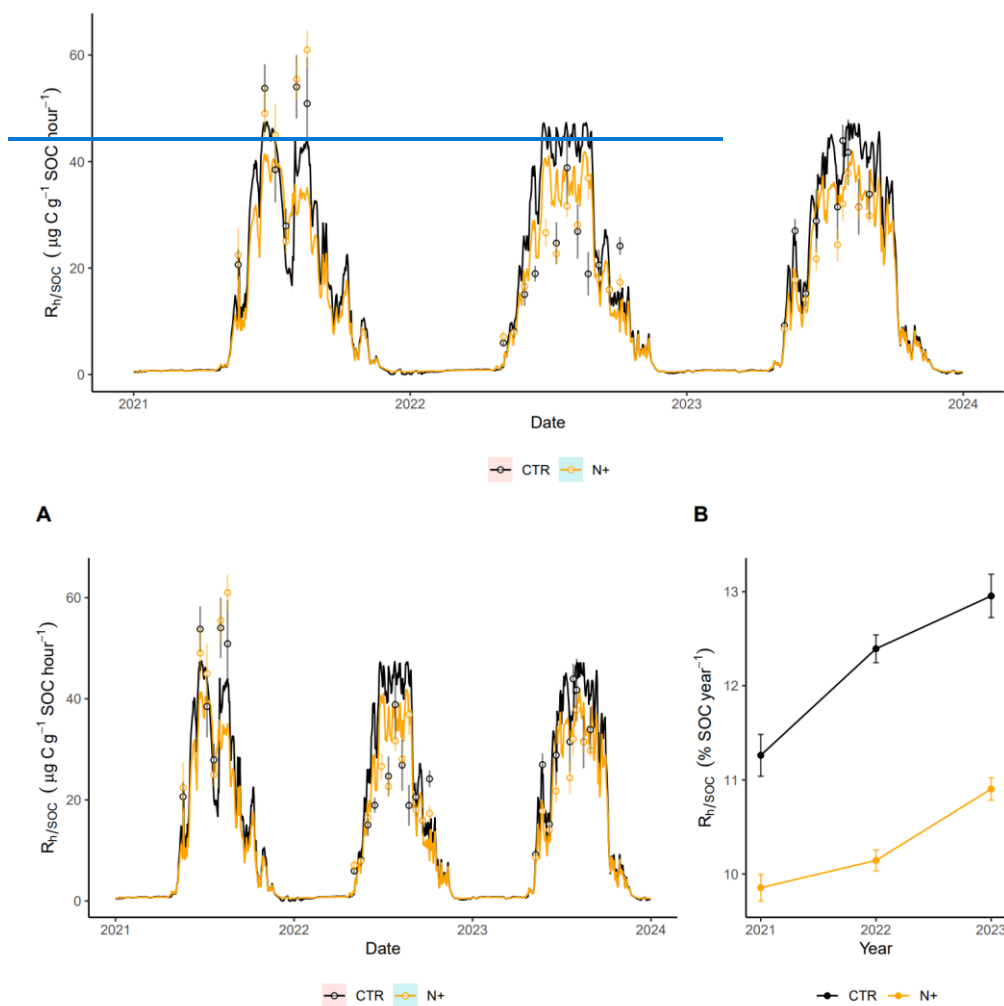
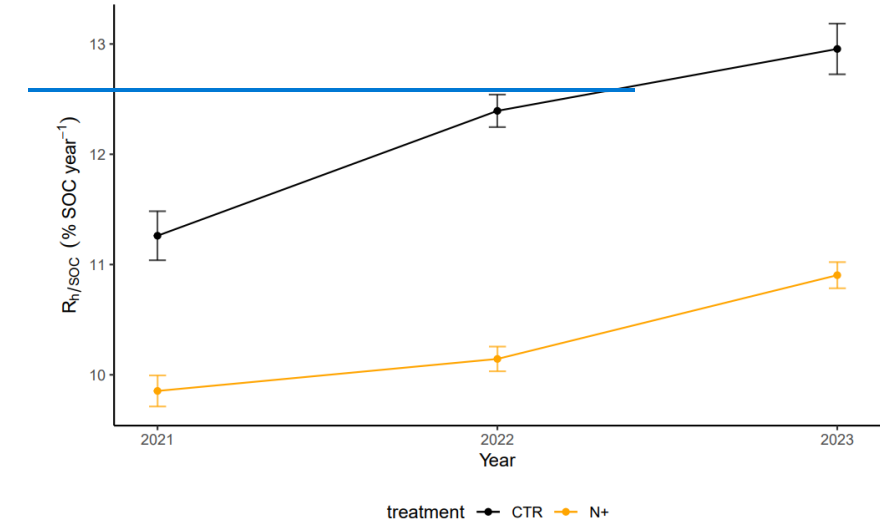


Figure 5: [A](#)) Time series of daily mean  $R_h/SOC$  ( $\mu\text{g C g}^{-1} \text{SOC h}^{-1}$ ) in CTR and N+ plots, with measurements shown as points (error bars indicate SE) and model estimates as lines (ribbons indicate SE). [B](#)) Annual  $R_h/SOC$  (% SOC per year) in CTR and N+ plots.

285 **3.5.4 Seasonal and annual differences in  $R_{hSOC}$  between CTR and N+ plots**

During the winter, daily model predictions of  $R_{hSOC}$  remained consistent across CTR and N+ treatments, with little variation due to low soil temperatures (Fig. 5a). However, in the summer, with temperatures above 5°C,  $R_{hSOC}$  modeled with combined-the function  $R_{hSOC}(T, SWC)$  displayed marked differences between CTR plots and N+ plots. In CTR plots, the modeled  $R_{hSOC}$  values were generally higher than in the N+ plots, except during a brief drought period in 2021, when modeled  $R_{hSOC}$  values decreased were lower. The  $R_{hSOC}(T, SWC)$  values of N+ plots in drought 2021 period also decreased. However, the daily  $R_{hSOC}$  modeled values of N+ were generally lower and showed less variation than in CTR plots, resulting in consistently lower annual  $R_{hSOC}$  in N+ than in CTR (Fig. 65b).



295 **Figure 6:** Annual  $R_{hSOC}$  (% SOC per year) estimated with NLS models driven by combined temperature and moisture ( $R_{hSOC}(T, SWC)$ , Eq. 1) in CTR and N+ plots, using hourly T and SWC data for model inputs (Fig. S1).

**3.6.5 Annual GWP reduction in relation to N addition**

As a result of the generally lower and less variable daily  $R_{hSOC}$  in N+ plots, the annual  $R_{hSOC}$  (expressed as % SOC respired per year) in N+ was also consistently lower than in CTR (Fig. 5b). Annual  $R_{hSOC}$  rates (expressed as % per unit SOC respired per year) based on daily model estimates ranged from 9.85 (±0.14 SE) % to 12.95 (±0.23 SE) % and increased over

during the 2021–2023 period (Fig. 65b). In CTR plots,  $R_{hSOC}(T, SWC)$  models yielded on average,  $R_{hSOC}(T, SWC)$  values were average 1.90 ( $\pm 0.41$  SE) % higher in control (CTR) plots compared to N-fertilized (N+) plots, rates than in N+ plots. This result suggests that, despite increased litter inputs in N+ plots due to enhanced tree growth, the relative decomposition rate per unit SOC remained unchanged or declined in fertilized plots, potentially favouring greater SOC retention. These results suggest that changes in sensitivity of annual  $R_{hSOC}$  to soil temperature and moisture in N+ plots contributes to SOC retention. The difference in modelled  $R_h$  (calculated as  $R_{hSOC}(T, SWC) \times SOC$ ) between CTR and N+ plots corresponds to a reduction of  $-345.4$  ( $\pm 73.6$  SE)  $g\ CO_2\ m^{-2}\ yr^{-1}$  in heterotrophic  $CO_2$  emissions (Table 3). The  $R_h$  rate ( $R_{hSOC}(T, SWC) \times SOC_{N+}$ ) difference between CTR and N+ showed potential reduction of  $CO_2$  emissions by  $-345.4$  ( $\pm 73.6$  SE)  $g\ CO_2\ m^{-2}\ yr^{-1}$  (Table 3). The GWP of reduced  $CH_4$  oxidation rates after N fertilization equaled to  $10.1$  ( $\pm 0.5$  SE)  $g\ CO_2\ eq\ m^{-2}\ yr^{-1}$ , and the increase in  $N_2O$  emissions to  $1.1$  ( $\pm 0.1$  SE)  $g\ CO_2\ eq\ m^{-2}\ yr^{-1}$  (Table 3). Thus, when considering the sum of these processes and the associated emissions with fertilizers productions  $6.5\ g\ CO_2\ m^{-2}\ yr^{-1}$ , the total GWP annual reduction in relation to N addition was  $-327.6$  ( $\pm 73.6$  SE)  $g\ CO_2\ m^{-2}\ yr^{-1}$ . This potential reduction in  $CO_2$  emissions outweighed the global warming potential (GWP) associated with increased  $N_2O$  emissions ( $1.1 \pm 0.1\ g\ CO_2\ eq\ m^{-2}\ yr^{-1}$ ), reduced  $CH_4$  uptake ( $10.1 \pm 0.5\ g\ CO_2\ eq\ m^{-2}\ yr^{-1}$ ) and fertilizer production emissions ( $6.5\ g\ CO_2\ eq\ m^{-2}\ yr^{-1}$ ). Overall, the net GWP balance suggests an annual reduction of  $-327.6$  ( $\pm 73.6$  SE)  $g\ CO_2\ eq\ m^{-2}\ yr^{-1}$  attributable to N fertilization.

Table 3: Annual global warming potential (GWP) reduction by long-term N fertilization in boreal Scots pine forest with contribution of individual greenhouse gas (GHG) fluxes (microbial respiration normalized by soil organic carbon stock  $R_{hSOC}$ ,  $CH_4$  net oxidation, and  $N_2O$  flux net exchange) evaluated as a difference between control (CTR) and N fertilized plots (N+). Minus values indicate net GWP reduction. The AR6 GWP-100 values 27 for  $CH_4$  and 273 for  $N_2O$  were used for calculation of  $CO_2$ -equivalents (ICCP, 2023). SE values were calculated considering variations across replicates and years together.

Treatment	$R_{hSOC}$		GWP- $CO_2$		$CH_4$		GWP- $CH_4$		$N_2O$		GWP- $N_2O$		GWP-GHG	
	(%)		( $g\ CO_2\ m^{-2}\ yr^{-1}$ )		( $g\ CH_4\ m^{-2}\ yr^{-1}$ )		( $g\ CO_2\ eq\ m^{-2}\ yr^{-1}$ )		( $mg\ N_2O\ m^{-2}\ yr^{-1}$ )		( $g\ CO_2\ eq\ m^{-2}\ yr^{-1}$ )		( $g\ CO_2\ eq\ m^{-2}\ yr^{-1}$ )	
	mean	SE	mean	SE	mean	SE	mean	SE	mean	SE	mean	SE	mean	SE
CTR	12.2	0.5	2214.9	90.4	-1.6	0.0	-42.9	0.5	-2.2	0.8	-0.6	0.2	2171.4	90.4
N+	10.3	0.3	1869.5	56.8	-1.2	0.0	-32.8	0.5	1.9	0.6	0.5	0.2	1837.3	56.8
Difference	-1.9	0.4	-345.4	73.6	0.4	0.0	10.1	0.5	4.2	0.7	1.1	0.2	-334.1	73.6



#### 4 Discussion

Our results show that nitrogen (N) fertilization significantly increased tree stand biomass and litterfall in N+ plots compared to control (CTR) plots (Fig. 2a), aligning with previous studies demonstrating enhanced forest productivity with N addition (Hyyönén et al., 2008). ~~The tree biomass reduction from 2014 to 2020, was due to~~ highlighted the strong impact of thinning in 2015 ~~and affected on aboveground carbon stocks and the~~ organic inputs to soil. Thinning corresponded to a litter input peak, with N+ plots showing higher litterfall than CTR. This ~~difference was further supported also with~~ confirmed by the above ground litterfall measurements during 2021-2023 ( $25.1 \text{ g m}^{-2} \text{ month}^{-1}$  in N+ vs.  $14.3 \text{ g m}^{-2} \text{ month}^{-1}$  in CTR) (Fig. 2b). Consistently with biomass and litterfall, soil organic carbon (SOC) increased under N fertilization, reaching  $5.6 \text{ kg C m}^{-2}$  in N+ compared to  $4.9 \text{ kg C m}^{-2}$  in CTR by 2023 (Fig. 2c), indicating enhanced SOC retention ~~alongside aboveground carbon storage due to reduced microbial respiration (Janssens et al., 2010); alongside aboveground carbon storage in the fertilized stands. Although, results from our study suggested a reduction in the  $R_{h/SOC}$  ratio, rather than an absolute decrease in  $R_h$ .~~

Differences in carbon stocks between treatments, prevented drawing conclusions on soil organic matter decomposition rates solely based on the observed increase in heterotrophic respiration ( $R_h$ ) under N fertilization (Fig. 3), and required normalizing respiration by SOC ( $R_{h/SOC}$ ). ~~When considering normalized respiration, we found a reduction in the annual  $R_{h/SOC}$  ratio, rather than an absolute decrease in  $R_h$ , with fertilization (Fig. 5b). This ratio~~ Normalizing respiration by SOC provides a meaningful way to interpret respiration rates relative to carbon availability, especially when comparing treatments with differing SOC stocks. ~~Although, this normalization~~ ~~ratio does not fully resolve the issue of  $R_h$  dependence on the amount of SOC, it has been widely adopted in field and incubation studies, as well as in soil carbon modeling frameworks (e.g., Tuomi et al., 2008; Davidson et al., 2012; Curiel Yuste et al., 2007; García-Angulo et al., 2020). Nonetheless,  $R_{h/SOC}$  should be interpreted with caution, as it does not capture underlying microbial mechanisms such as enzyme kinetics or community structure, which introduce nonlinearities in the decomposition kinetics. Whereas (normalizing  $R_h$  by SOC as a proxy of the decomposition rate constant assumes a linear relation between decomposition rate and SOC). In the absence of microbial process data, it serves as a useful, though imperfect, indicator of decomposition efficiency rates.~~

Although, the ~~daily measured~~ mean  $R_{h/SOC}$  values were not statistically different between CTR and N+ ~~and~~ ~~the~~  $R_{h/SOC}$  responded to N fertilization with reduced sensitivity to soil moisture (Fig. 4), suggesting a potential mechanism (e.g., ~~microbial adaptation~~, substrate shifts) for enhanced carbon retention in fertilized plots. However, the slightly increased sensitivity of microbial respiration to temperature at higher values in N fertilized plots (Fig. 4a) may indicate a risk of accelerated carbon loss under warming conditions in the ~~fertilized~~ soils compared to controls. This dual response to long-term N fertilization, which are discussed in detail in following ~~chapters~~, highlights the need to consider both moisture and temperature responses in models predicting boreal forest soil carbon dynamics in the context of long-term atmospheric N deposition, ~~fertilization~~,s and climate change.

360

#### 4.1 Response of soil heterotrophic respiration to N fertilization

The meta-analysis of  $R_h$  responses to N fertilization in temperate and boreal forests, reported a 15% average decrease in heterotrophic  $CO_2$  emissions (Janssens et al., 2010). However, the wide range of responses of heterotrophic  $CO_2$  emissions following N fertilization (~~Janssens et al., 2010~~), spanning from a 57% decrease to a 63% increase, encompasses 26% increase in mean soil heterotrophic respiration ( $R_h$ ) from 2021–2023, observed here (Fig. 3a). Limiting  $R_h$  by N fertilization in low-productivity forests (Janssens et al., 2010) may relate to low litter quality, as observed in our study's *Calluna*- and *Vaccinium vitis idaea*-type Scots pine forest.

370

Yet, higher litter amount due to higher biomass production and thinning in fertilized (N+) than in control (CTR) plots (Fig. 2a and Fig. 2b) may support increased  $R_h$  in N+. Although thinning effects on boreal Scots pine  $R_h$  are generally modest (Aun et al., 2021), larger inputs of higher-quality litter from harvest residues in N+ plots, including fine roots, needles, and branches, likely stimulated  $R_h$  (Liski et al., 2006; Zhang et al., 2018). This enhanced carbon availability, along with increased soil nitrogen concentrations, and stimulated microbial activity and biopolymers degradation capabilities explains the observed increase in ~~heterotrophic respiration ( $R_h$ )~~ under N fertilization (Fig. 3). Additionally, we observed a decline in phosphorus concentrations in N-fertilized plots compared to unfertilized plots, probably due to microorganisms mining for phosphorus to sustain their increased activity (Richy et al., 2024).

380 Despite the significant increase in [daily measured  \$R\_h\$](#) , [the daily measured](#) SOC-normalized heterotrophic respiration ( $R_{h/SOC}$ ) did not differ significantly between CTR and N+ plots [but at the annual scale  \$R\_{h/SOC}\$  differed](#). This suggests that increased  $R_h$  with N addition originated more from higher litter input and SOC rather than an enhanced microbial decomposition rates (Fig. 3b). The  $R_h$  responses to N in Sweden's Rosinedalsheden Scots pine forest also showed variability, with differing results based on plot size and SOC pool similarity (Hasselquist et al., 2012; Marshall et al., 2021). Using hourly  $R_{h/SOC}$  (Curiel Yuste et al., 2007; Shahbaz et al., 2022) may better capture decomposition rate differences than  $R_h$  alone, yet hourly-scale  $R_{h/SOC}$  responses to N fertilization may still be obscured by fine-scale spatial and temporal variations in soil temperature and moisture (Fig. 3, Fig. S2), primary drivers of  $R_{h/SOC}$  (Curiel Yuste et al., 2007; Shahbaz et al., 2022). For example, our biweekly measurements of  $R_{h/SOC}$  showed similar means for CTR and N+ plots, but annual  $R_{h/SOC}$  means differed (Fig. 6), reflecting differences in temperature and moisture distribution and differences in functional  $R_{h/SOC}$  dependencies to temperature and moisture between treatments (Fig. S1 and Fig. S2; Fig. 4).

390

#### 4.2 Shifts in $R_h$ dependency on soil environmental conditions with N addition

The functional relationships between  $R_h$  and environmental variables such as soil temperature (T) and volumetric soil water content (SWC), used in Earth system and soil C models (Falloon et al., 2011; Sierra et al., 2015), often overlook soil N status. Earth system models often relate  $R_h$  to T and SWC, but commonly ignore how the soil N status could modulate such T and SWC responses (Falloon et al., 2011; Sierra et al., 2015). Here, we observed that N fertilization modified the  $R_{h/SOC}$  dependency on both T and SWC, with a sharper increase in  $R_{h/SOC}$  with temperature in N+ plots relative to CTR plots. Unlike CTR plots, where  $R_{h/SOC}$  declined at temperatures above 15 °C, N+ plots maintained elevated  $R_{h/SOC}$  values under high temperatures (Fig. 4a) which is in line with Chen et al. (2024) and may in warming climates indicate higher risk of increased CO<sub>2</sub> emissions from accumulated SOC in warming climates. This increased  $R_{h/SOC}$  at high temperature in response to N addition could be attributed to shifts in substrate composition, where N fertilization enhances the decomposition of labile, C-rich litter (high N availability increases C demand by microbes) and suppresses the decomposition of N-rich organic matter with high lignin content (due to decreased N demand) (Berg and Matzner, 1997; Bonner et al., 2019; Janssens et al., 2010; Wu et al., 2023). Furthermore, our study site exhibited increased Mn peroxidase activity following long-term N addition, indicating enhanced microbial degradation of polyphenolic compounds (Richy et al., 2024). Thus, shifts in litter quality, specifically C and N ratios, likely contribute to divergent  $R_h$  responses to temperature (Robinson et al., 2020).

Moisture also plays a pivotal role in  $R_h$  sensitivity to temperature (Robinson et al., 2020), and in modifying soil respiration rates especially under N fertilization and drought conditions (Nair et al., 2024). In our N-fertilized plots,  $R_{h/SOC}$  was largely independent of soil moisture, and contrasted with the expected humped response of  $R_{h/SOC}$  to SWC in CTR plots (Fig. 4b). This variation in SWC response suggests potential microbial adaptation to moisture availability (Lennon et al., 2012; Manzeni et al., 2024) and changes in soil physical properties influencing O<sub>2</sub> and solute diffusivity (Huang et al., 2023; Moyano et al., 2013). However, the lack of significance of the moisture shape parameter  $c$  in the N-fertilized treatment (Table 1) reflected both variability in the data and the absence of a distinct moisture optimum. The contrast between the flat response to moisture in N+ and clear peaked moisture response in CTR highlights potential treatment-related shifts in environmental sensitivity, but also underscores the need to interpret model-based extrapolations with caution. The observed differences between CTR and N+ plots could imply that N status or fertilization-induced changes in soil properties influence the sensitivity of organic matter decomposition to moisture. Soil moisture influences microbial carbon use efficiency (CUE) by affecting substrate accessibility and physiological stress, with lower CUE observed in dry soils (Butcher et al., 2020; Ullah et al., 2021). However, in our study differences in CUE could not be directly inferred from our data, as microbial process measurements were not conducted. Additionally, accelerated decomposition following soil rewetting, commonly referred to as the “Birch effect,” has been linked to increased short term N availability (Jarvis et al., 2007). However, prolonged N addition may impose a phosphorus limitation on decomposition due to N imbalance (Richy et al., 2024).

Simulating  $R_{hSOC}$  based on both temperature and moisture inputs showed that models relying solely on temperature underestimate  $R_{hSOC}$  for initially N-limited boreal forest soils (Fig. 5 and Fig. 6). Thus, current soil C models ~~should-could~~ integrate both temperature and moisture dependencies in their environmental modifiers of decomposition rates, as well as consider variations in SWC response under differing N statuses to improve SOC accuracy in fertile soils (Tupek et al., 2016).

For example, the CENTURY model (Parton et al., 1987), which considers topsoil N content and its effect on the fine-litter C ratio, ~~offers-predicts~~ a slight increase in simulated SOC stocks (Tupek et al., 2016), whereas ~~other models like-g.~~ Yasso model (Tuomi et al., 2011) ~~does~~ not account for soil N. However, by restricting topsoil N effects solely to ~~linear-scaling-of carbon-use-efficiency-(CUE)~~ or decomposition rates (Zhang et al., 2018), current models lack the ability to capture the influence of N-driven variations in temperature and moisture modifiers. This limitation highlights the need to re-evaluate the ~~linear~~-scaling of decomposition with N to better account for the differential respiration sensitivities observed in this study (Fig. 4). Incorporating nonlinear nitrogen effects on temperature and soil moisture modifiers depends on the model's structure. In soil carbon-only models like Yasso, updating these modifiers with a larger dataset that includes nitrogen deposition gradients and soil organic carbon stocks could improve performance. Conversely, in soil carbon-nitrogen models that already account for SOC-N interactions, existing functional relationships should be re-evaluated, considering their interactions with environmental modifiers.

### 4.3 Implications for climate change mitigation

~~Annually, N-fertilized plots respired 10.3% of SOC ( $\pm 0.3$  SE), compared to 12.2% ( $\pm 0.5$  SE) in CTR plots, indicating that N-fertilization increased microbial C-use efficiency, leading to SOC accumulation. Annually, N-fertilized plots respired 10.3% of SOC ( $\pm 0.3$  SE), compared to 12.2% ( $\pm 0.5$  SE) in CTR plots. Although the difference was derived from the modeled values, the lower respiration rate in fertilized plots suggests a potential increase in microbial carbon-use efficiencyCUE, which may contribute to long-term SOC accumulation. Despite the winter fluxes not being directly measured, modeled values under low soil temperatures ( $<5^\circ\text{C}$ ) were close to zero for both treatments due to strong temperature limitation observed in measured data. As a result, differences in winter  $R_{hSOC}$  contributed minimally to annual estimates and are unlikely to have significantly biased treatment comparisons.~~ This 1.90 ( $\pm 0.41$  SE) % reduction in annual SOC loss due to N addition corresponds to an average of 345.4 ( $\pm 73.6$  SE) g  $\text{CO}_2 \text{ m}^{-2} \text{ yr}^{-1}$ . The combined effect of reduced methane ( $\text{CH}_4$ ) oxidation and a slight shift in nitrous oxide ( $\text{N}_2\text{O}$ ) from a sink to an emitter comparable to Maljanen et al., (2006), and equivalent to 8.7 g  $\text{CO}_2\text{eq. m}^{-2} \text{ year}^{-1}$  did not negate this positive mitigation potential and agreed with Öquist et al., (2024). The Haber-Bosch process required for  $\text{N}_2$  to  $\text{NH}_3$  conversion has an associated emission cost of approximately 2.96 kg  $\text{CO}_2\text{eq. per kg NH}_3$  (Osorio-Tejada et al., 2022), which would reduce our calculated mitigation potential by about 6.5 g  $\text{CO}_2 \text{ m}^{-2} \text{ year}^{-1}$ . Consequently, the average mitigation potential for N fertilization in our forest soil study is estimated at -327.6  $\pm 73.6$  SE g  $\text{CO}_2 \text{ m}^{-2} \text{ yr}^{-1}$  (equivalent to 0.89  $\pm 0.2$  SE -t C  $\text{ha}^{-1} \text{ year}^{-1}$ ). The estimated net GHG mitigation of -327.6 g  $\text{CO}_2 \text{ m}^{-2} \text{ yr}^{-1}$  based on  $R_{hSOC}$  model outputs from a three-year period provides a first-order approximation. However, this estimate likely underrepresents the full climate impact of fertilization, as it does not account for longer-term dynamics or

potential offsite C and N losses, such as leaching, indirect emissions, or biodiversity-related feedback. Therefore, broader system-level assessments over longer time scales are needed to confirm these findings. While these findings likely apply to a nutrient-poor boreal ecosystems, extrapolation ~~should be done for to~~ similar stands with similar climate ~~—and even more to other ecosystems—should be done~~ with caution ~~for other ecosystems~~. For example, Saarsalmi et al. (2014) showed that N fertilization stimulated ~~growth in relation to~~ mean annual production (more in nutrient poor pine stands and less in spruce stands with higher nutrient status). Schulte-Uebbing et al. (2021) demonstrated that N addition enhance biomass carbon sequestration primarily in boreal regions, while having negative effects in tropical forests.

## 5 Conclusions

Although our experiment design allowed exploratory insights into N fertilization effects, caution is needed in extrapolating beyond this site. While results represent a case study, This study they reveals that increased soil N status after long-term N fertilization in boreal Scots pine ecosystems can alter the dependency of C decomposition on temperature and moisture. Although the models showed relatively large mean residuals when evaluated against individual measurements, their mean bias errors were close to zero. Incorporating these findings into soil C models suggests global implications for reducing uncertainty of boreal soil CO<sub>2</sub> emission estimates and soil C stock projections under N deposition and climate warming. Our resultsThe results also suggest a net reduction in soil GHG emissions with long-term N fertilization, indicating that N fertilization in our boreal Scots pine ecosystems-forest not only enhances-enhanced tree biomass but may also serve-acted as a viable forest management strategy for climate change mitigation.

## References

Aun, K., Kukumägi, M., Varik, M., Becker, H., Aosaar, J., Uri, M., Morozov, G., Buht, M., Uri, V.: Short-term effect of thinning on the carbon budget of young and middle-aged Scots pine (*Pinus sylvestris* L.) stands, Forest Ecology and Management, 492, 119241, <https://doi.org/10.1016/j.foreco.2021.119241>, 2021.

Berg, B., Matzner, E.: Effect of N deposition on decomposition of plant litter and soil organic matter in forest systems, Environmental Reviews, 5, 1–25, <https://doi.org/10.1139/a96-017>, 1997.

Bolker, B. M.: Ecological Models and Data in R, Princeton University Press, <https://doi.org/10.1515/9781400840908>, 2008.

Bonner, M. T. L., Castro, D., Schneider, A. N., Sundström, G., Hurry, V., Street, N. R., Näsholm, T.: Why does nitrogen addition to forest soils inhibit decomposition?, Soil Biology and Biochemistry, 137, 107570, <https://doi.org/10.1016/j.soilbio.2019.107570>, 2019.

Butcher, K. R., Nasto, M. K., Norton, J. M., Stark, J. M.: Physical mechanisms for soil moisture effects on microbial carbon-use efficiency in a sandy loam soil in the western United States, *Soil Biology and Biochemistry*, 150, 107969, <https://doi.org/10.1016/j.soilbio.2020.107969>, 2020.

Cajander, A. K.: Forest types and their significance, *Acta Forestalia Fennica*, 56, 1949.

Chen, C., Pei, J., Li, B., Fang, C., Nie, M., Li, J.: Nutrient Addition Enhances the Temperature Sensitivity of Soil Carbon Decomposition Across Forest Ecosystems. *Global Change Biology* 30, e17543. <https://doi.org/10.1111/gcb.17543>, 2024.

Curiel Yuste, J., Baldocchi, D. D., Gershenson, A., Goldstein, A., Misson, L., Wong, S.: Microbial soil respiration and its dependency on carbon inputs, soil temperature and moisture, *Global Change Biology*, 13, 2018–2035, <https://doi.org/10.1111/j.1365-2486.2007.01415.x>, 2007.

Craine, J.M., Morrow, C. and Fierer, N.: Microbial nitrogen limitation increases decomposition. *Ecology*, 88, 2105–2113, <https://doi.org/10.1890/06-1847.1>, 2007.

Dalsgaard, L., Lange, H., Strand, L. T., Callesen, I., Borgen, S. K., Liski, J., Astrup, R.: Underestimation of boreal forest soil carbon stocks related to soil classification and drainage, *Canadian Journal of Forest Research*, 46, 1413–1425, <https://doi.org/10.1139/cjfr-2015-0466>, 2016.

DeLuca, T. H., Boisvenue, C.: Boreal forest soil carbon: distribution, function and modelling, *Forestry*, 85, 161–184, <https://doi.org/10.1093/forestry/cps003>, 2012.

Eriksson, C. P., Holmgren, P.: Estimating stone and boulder content in forest soils — evaluating the potential of surface penetration methods, *CATENA*, 28, 121–134, [https://doi.org/10.1016/S0341-8162\(96\)00031-8](https://doi.org/10.1016/S0341-8162(96)00031-8), 1996.

Falloon, P., Jones, C. D., Ades, M., and Paul, K.: Direct soil moisture controls of future global soil carbon changes: An important source of uncertainty, *Global Biogeochemical Cycles*, 25, GB3010, <https://doi.org/10.1029/2010GB003938>, 2011.

García-Angulo, D., Hereş, A.-M., Fernández-López, M., Flores, O., Sanz, M.J., Rey, A., Valladares, F., and Curiel Yuste, J.: Holm Oak Decline and Mortality Exacerbates Drought Effects on Soil Biogeochemical Cycling and Soil Microbial Communities across a Climatic Gradient, *Soil Biology and Biochemistry*, 149, <https://doi.org/10.1016/j.soilbio.2020.107921>, 2020.

Hasselquist, N. J., Metcalfe, D. B., and Höglberg, P.: Contrasting effects of low and high nitrogen additions on soil CO<sub>2</sub> flux components and ectomycorrhizal fungal sporocarp production in a boreal forest, *Global Change Biology*, 18, 3596–3605, <https://doi.org/10.1111/j.1365-2486.2012.02788.x>, 2012.

Höglberg, P., Näsholm, T., Franklin, O., and Höglberg, M. N.: Tamm Review: On the nature of the nitrogen limitation to plant growth in Fennoscandian boreal forests, *Forest Ecology and Management*, 403, 161–185, <https://doi.org/10.1016/j.foreco.2017.04.045>, 2017.

Huang, Z., Liu, Y., Huang, P., Li, Z., and Zhang, X.: A new concept for modelling the moisture dependence of heterotrophic soil respiration, *Soil Biology and Biochemistry*, 185, 109147, <https://doi.org/10.1016/j.soilbio.2023.109147>, 2023.

520 Hyvönen, R., Persson, T., Andersson, S., Olsson, B., Ågren, G. I., and Linder, S.: Impact of long-term nitrogen addition on carbon stocks in trees and soils in Northern Europe, *Biogeochemistry*, 89, 121–137, <https://doi.org/10.1007/s10533-008-9210-3>, 2008.

Intergovernmental Panel On Climate Change (Ipcc), 2023. Climate Change 2021 – The Physical Science Basis: Working Group I Contribution to the Sixth Assessment Report of the Intergovernmental Panel on Climate Change, 1st ed. Cambridge University Press. <https://doi.org/10.1017/9781009157896>

525 Janssens, I. A., Dieleman, W., Luyssaert, S., Subke, J.-A., Reichstein, M., Ceulemans, R., Ciais, P., Dolman, A. J., Grace, J., Matteucci, G., Papale, D., Piao, S. L., Schulze, E.-D., Tang, J., and Law, B. E.: Reduction of forest soil respiration in response to nitrogen deposition, *Nature Geoscience*, 3, 315–322, <https://doi.org/10.1038/ngeo844>, 2010.

Jarvis, P. and Linder, S.: Constraints to growth of boreal forests, *Nature*, 405, 904–905, <https://doi.org/10.1038/35016154>, 530 2000.

Jarvis, P., Rey, A., Petsikos, C., Wingate, L., Rayment, M., Pereira, J., Banza, J., David, J., Miglietta, F., Borghetti, M., Manca, G., and Valentini, R.: Drying and wetting of Mediterranean soils stimulates decomposition and carbon dioxide emission: The “Birch effect,” *Tree Physiology*, 27, 929–940, <https://doi.org/10.1093/treephys/27.7.929>, 2007.

Khurana, S., Abramoff, R., Bruni, E., Dondini, M., Tupek, B., Guenet, B., Lehtonen, A., and Manzoni, S.: Interactive effects of microbial functional diversity and carbon availability on decomposition – A theoretical exploration, *Ecological Modelling*, 486, 110507, <https://doi.org/10.1016/j.ecolmodel.2023.110507>, 2023.

535 Kuhn, M.: Building predictive models in R using the caret package, *Journal of Statistical Software*, 28, 1–26, <https://doi.org/10.18637/jss.v028.i05>, 2008.

Lehtonen, A., Linkosalo, T., Peltoniemi, M., Sievänen, R., Mäkipää, R., Tamminen, P., Salemaa, M., Nieminen, T., Tupek, B., Heikkinen, J., and Komarov, A.: Forest soil carbon stock estimates in a nationwide inventory: Evaluating performance of the ROMULv and Yasso07 models in Finland, *Geoscientific Model Development*, 9, 4169–4183, <https://doi.org/10.5194/gmd-9-4169-2016>, 2016.

Lennon, J. T., Aanderud, Z. T., Lehmkuhl, B. K., and Schoolmaster Jr., D. R.: Mapping the niche space of soil microorganisms using taxonomy and traits, *Ecology*, 93, 1867–1879, <https://doi.org/10.1890/11-1745.1>, 2012.

545 Liski, J., Lehtonen, A., Palosuo, T., Peltoniemi, M., Eggers, T., Muukkonen, P., and Mäkipää, R.: Carbon accumulation in Finland’s forests 1922–2004 – An estimate obtained by combination of forest inventory data with modelling of biomass, litter, and soil, *Annals of Forest Science*, 63, 687–697, <https://doi.org/10.1051/forest:2006049>, 2006.

Luo, Y., Ahlström, A., Allison, S. D., Batjes, N. H., Brovkin, V., Carvalhais, N., Chappell, A., Ciais, P., Davidson, E. A., Finzi, A., Georgiou, K., Guenet, B., Hararuk, O., Harden, J. W., He, Y., Hopkins, F., Jiang, L., Koven, C., Jackson, R. B., Jones, C. D., Lara, M. J., Liang, J., McGuire, A. D., Parton, W., Peng, C., Randerson, J. T., Salazar, A., Sierra, C. A., Smith, M. J., Tian, H., Todd-Brown, K. E. O., Torn, M., Groenigen, K. J. van, Wang, Y. P., West, T. O., Wei, Y., Wieder, W. R., Xia, J., Xu, X., and Zhou, T.: Toward more realistic projections of soil carbon dynamics by Earth system models, *Global Biogeochemical Cycles*, 30, 40–56, <https://doi.org/10.1002/2015GB005239>, 2016.

Lupi, C., Morin, H., Deslauriers, A., Rossi, S., and Houle, D.: Role of soil nitrogen for the conifers of the boreal forest: A critical review, *International Journal of Plant and Soil Science*, 155–189, <https://doi.org/10.9734/IJPSS/2013/4233>, 2013

555 Machacova, K., Bäck, J., Vanhatalo, A., Halmeenmäki, E., Kolari, P., Mammarella, I., Pumpanen, J., Acosta, M., Urban, O., and Pihlatie, M.: *Pinus sylvestris* as a missing source of nitrous oxide and methane in boreal forest, *Scientific Reports*, 6, 23410, <https://doi.org/10.1038/srep23410>, 2016.

Mäkipää, R., Abramoff, R., Adamczyk, B., Baldy, V., Biryol, C., Bosela, M., Casals, P., Yuste, J. C., Dondini, M., Filipek, S., et al.: How does management affect soil C sequestration and greenhouse gas fluxes in boreal and temperate forests? – A review, *Forest Ecology and Management*, 529, 120637, <https://doi.org/10.1016/j.foreco.2023.120637>, 2023.

560 Manzoni, S., Čapek, P., Mooshammer, M., Lindahl, B. D., Richter, A., and Šantrůčková, H.: Optimal metabolic regulation along resource stoichiometry gradients, *Ecology Letters*, 20, 1182–1191, <https://doi.org/10.1111/ele.12815>, 2017.

Manzoni, S., Chakrawal, A., Spohn, M., and Lindahl, B. D.: Modeling microbial adaptations to nutrient limitation during litter decomposition, *Frontiers in Forests and Global Change*, 4, <https://doi.org/10.3389/ffgc.2021.663432>, 2021.

565 Manzoni, S., Schimel, J. P., and Porporato, A.: Responses of soil microbial communities to water stress: Results from a meta-analysis, *Ecology*, 93, 930–938, <https://doi.org/10.1890/11-0026.1>, 2012a.

Manzoni, S., Taylor, P., Richter, A., Porporato, A., and Ågren, G. I.: Environmental and stoichiometric controls on microbial carbon-use efficiency in soils, *New Phytologist*, 196, 79–91, <https://doi.org/10.1111/j.1469-8137.2012.04225.x>, 2012b.

570 Maljanen, M., Jokinen, H., Saari, A., Strömmer, R., and Martikainen, P. J.: Methane and nitrous oxide fluxes, and carbon dioxide production in boreal forest soil fertilized with wood ash and nitrogen, *Soil Use and Management*, 22, 151–157, <https://doi.org/10.1111/j.1475-2743.2006.00029.x>, 2006.

Marshall, J. D., Peichl, M., Tarvainen, L., Lim, H., Lundmark, T., Näsholm, T., Öquist, M., and Linder, S.: A carbon-budget approach shows that reduced decomposition causes the nitrogen-induced increase in soil carbon in a boreal forest, *Forest Ecology and Management*, 502, 119750, <https://doi.org/10.1016/j.foreco.2021.119750>, 2021.

575 Matson, A., Pennock, D., and Bedard-Haughn, A.: Methane and nitrous oxide emissions from mature forest stands in the boreal forest, Saskatchewan, Canada, *Forest Ecology and Management*, 258, 1073–1083, <https://doi.org/10.1016/j.foreco.2009.05.034>, 2009.

580 Mayer, M., Prescott, C. E., Abaker, W. E. A., Augusto, L., Cécillon, L., Ferreira, G. W. D., James, J., Jandl, R., Katzensteiner, K., Laclau, J.-P., et al.: Tamm Review: Influence of forest management activities on soil organic carbon stocks: A knowledge synthesis, *Forest Ecology and Management*, 466, 118127, <https://doi.org/10.1016/j.foreco.2020.118127>, 2020.

Moyano, F. E., Manzoni, S., and Chenu, C.: Responses of soil heterotrophic respiration to moisture availability: An exploration of processes and models, *Soil Biology and Biochemistry*, 59, 72–85, <https://doi.org/10.1016/j.soilbio.2013.01.002>, 2013.



Moyano, F. E., Vasilyeva, N., Bouckaert, L., Cook, F., Craine, J., Curiel Yuste, J., Don, A., Epron, D., Formanek, P., Franzluebbers, A., et al.: The moisture response of soil heterotrophic respiration: Interaction with soil properties, *Biogeosciences*, 9, 1173–1182, <https://doi.org/10.5194/bg-9-1173-2012>, 2012.

Muukkonen, P., Häkkinen, M., and Mäkipää, R.: Spatial variation in soil carbon in the organic layer of managed boreal forest soil—implications for sampling design, *Environmental Monitoring and Assessment*, 158, 67–76, <https://doi.org/10.1007/s10661-008-0565-2>, 2009.

Nair, R., Luo, Y., El-Madany, T., Rolo, V., Pacheco-Labrador, J., Caldararu, S., Morris, K. A., Schrumpf, M., Carrara, A., Moreno, G., et al.: Nitrogen availability and summer drought, but not N:P imbalance, drive carbon use efficiency of a Mediterranean tree-grass ecosystem, *Global Change Biology*, 30, e17486, <https://doi.org/10.1111/gcb.17486>, 2024.

Näsholm, T., Ekblad, A., Nordin, A., Giesler, R., Höglberg, M., and Höglberg, P.: Boreal forest plants take up organic nitrogen, *Nature*, 392, 914–916, <https://doi.org/10.1038/31921>, 1998.

Öquist, M. G., He, H., Bortolazzi, A., Nilsson, M. B., Rodeghiero, M., Tognetti, R., Ventura, M., and Egnell, G.: Nitrogen fertilization increases N<sub>2</sub>O emission but does not offset the reduced radiative forcing caused by the increased carbon uptake in boreal forests, *Forest Ecology and Management*, 556, 121739, <https://doi.org/10.1016/j.foreco.2024.121739>, 2024.

Ortiz, C. A., Liski, J., Gärdenäs, A. I., Lehtonen, A., Lundblad, M., Stendahl, J., Ågren, G. I., and Karlton, E.: Soil organic carbon stock changes in Swedish forest soils—A comparison of uncertainties and their sources through a national inventory and two simulation models, *Ecological Modelling*, 251, 221–231, <https://doi.org/10.1016/j.ecolmodel.2012.12.017>, 2013.

Osorio-Tejada, J., Tran, N.N., Hessel, V.: Techno-environmental assessment of small-scale Haber-Bosch and plasma-assisted ammonia supply chains. *Science of The Total Environment* 826, 154162, <https://doi.org/10.1016/j.scitotenv.2022.154162>, 2022.

Pallandt, M., Ahrens, B., Koirala, S., Lange, H., Reichstein, M., Schrumpf, M., and Zachle, S.: Vertically Divergent Responses of SOC Decomposition to Soil Moisture in a Changing Climate, *Journal of Geophysical Research: Biogeosciences*, 127, e2021JG006684, <https://doi.org/10.1029/2021JG006684>, 2022.

Parkin, T.B., Venterea, R.T., Hargreaves, S.K.: Calculating the detection limits of chamber-based soil greenhouse gas flux measurements. *J. Environ. Qual.* 41, 705–715, <https://doi.org/10.2134/jeq2011.0394>, 2012.

Pihlatie, M., Pumpanen, J., Rinne, J., Ilvesniemi, H., Simojoki, A., Hari, P., and Vesala, T.: Gas concentration driven fluxes of nitrous oxide and carbon dioxide in boreal forest soil, *Tellus B: Chemical and Physical Meteorology*, 59, 458–469, <https://doi.org/10.1111/j.1600-0889.2007.00278.x>, 2007.

Parton, W.J., Schimel, D.S., Cole, C.V., and Ojima, D.S.: Analysis of factors controlling soil organic matter levels in Great Plains grasslands. *Soil Science Society of America Journal*, 51, 1173–1179, <https://doi.org/10.2136/sssaj1987.03615995005100050015x>, 1987.

Poepplau, C., Vos, C., and Don, A.: Soil organic carbon stocks are systematically overestimated by misuse of the parameters bulk density and rock fragment content, *SOIL*, 3, 61–66, <https://doi.org/10.5194/soil-3-61-2017>, 2017.

- Repola, J.: Biomass equations for Scots pine and Norway spruce in Finland, *Silva Fennica*, 43, <https://doi.org/10.14214/sf.184>, 2009.
- Richy, E., Fort, T., Odriozola, I., Kohout, P., Barbi, F., Martinovic, T., Tupek, B., Adamczyk, B., Lehtonen, A., Mäkipää, R., and Baldrian, P.: Phosphorus limitation promotes soil carbon storage in a boreal forest exposed to long-term nitrogen fertilization, *Global Change Biology*, 30, e17516, <https://doi.org/10.1111/gcb.17516>, 2024.
- Robinson, J. M., Barker, S. L. L., Arcus, V. L., McNally, S. R., and Schipper, L. A.: Contrasting temperature responses of soil respiration derived from soil organic matter and added plant litter, *Biogeochemistry*, 150, 45–59, <https://doi.org/10.1007/s10533-020-00686-3>, 2020.
- Saarsalmi, A., and Mälkönen, E.: Forest Fertilization Research in Finland: A Literature Review, *Scandinavian Journal of Forest Research*, 16, 514–535, <https://doi.org/10.1080/02827580152699358>, 2001.
- Sakamoto, Y., Ishiguro, M., and Kitagawa, G.: Akaike Information Criterion Statistics, D. Reidel Publishing Company, Dordrecht, 1986.
- Schulte-Uebbing, L.F., Ros, G.H., de Vries, W., 2022. Experimental evidence shows minor contribution of nitrogen deposition to global forest carbon sequestration. *Global Change Biology* 28, 899–917. <https://doi.org/10.1111/gcb.15960>
- Shahbaz, M., Bengtson, P., Mertes, J. R., Kulessa, B., and Kljun, N.: Spatial heterogeneity of soil carbon exchanges and their drivers in a boreal forest, *Science of the Total Environment*, 831, 154876, <https://doi.org/10.1016/j.scitotenv.2022.154876>, 2022.
- Sierra, C. A., Malghani, S., and Loescher, H. W.: Interactions among temperature, moisture, and oxygen concentrations in controlling decomposition rates in a boreal forest soil, *Biogeosciences*, 14, 703–710, <https://doi.org/10.5194/bg-14-703-2017>, 2017.
- Sierra, C. A., Trumbore, S. E., Davidson, E. A., Vicca, S., and Janssens, I. A.: Sensitivity of decomposition rates of soil organic matter with respect to simultaneous changes in temperature and moisture, *Journal of Advances in Modeling Earth Systems*, 7, 335–356, <https://doi.org/10.1002/2014MS000358>, 2015.
- Siljanen, H. M. P., Welti, N., Voigt, C., Heiskanen, J., Biasi, C., and Martikainen, P. J.: Atmospheric impact of nitrous oxide uptake by boreal forest soils can be comparable to that of methane uptake, *Plant and Soil*, 454, 121–138, <https://doi.org/10.1007/s11104-020-04638-6>, 2020.
- Smolander, A., Kurka, A., Kitunen, V., and Mälkönen, E.: Microbial biomass C and N, and respiratory activity in soil of repeatedly limed and N- and P-fertilized Norway spruce stands, *Soil Biology and Biochemistry*, 26, 957–962, [https://doi.org/10.1016/0038-0717\(94\)90109-0](https://doi.org/10.1016/0038-0717(94)90109-0), 1994.
- Sponseller, R. A., Gundale, M. J., Futter, M., Ring, E., Nordin, A., Näsholm, T., and Laudon, H.: Nitrogen dynamics in managed boreal forests: Recent advances and future research directions, *Ambio*, 45, 175–187, <https://doi.org/10.1007/s13280-015-0755-4>, 2016.

Tuomi, M., Vanhala, P., Karhu, K., Fritze, H., and Liski, J.: Heterotrophic soil respiration—Comparison of different models describing its temperature dependence, *Ecological Modelling*, 211, 182–190, <https://doi.org/10.1016/j.ecolmodel.2007.09.003>, 2008.

Tuomi, M., Laiho, R., Repo, A., and Liski, J.: Wood decomposition model for boreal forests. *Ecological Modelling*, 222, 709–718, <https://doi.org/10.1016/j.ecolmodel.2010.10.025>, 2011.

Tupek, B., Minkinen, K., Kolari, P., Starr, M., Chan, T., Alm, J., Vesala, T., and Nikinmaa, E.: Forest floor versus ecosystem CO<sub>2</sub> exchange along boreal ecotone between upland forest and lowland mire, *Tellus B: Chemical and Physical Meteorology*, 60, 153–166, <https://doi.org/10.1111/j.1600-0889.2007.00328.x>, 2008.

Tupek, B., Minkinen, K., Pumpanen, J., Vesala, T., and Nikinmaa, E.: CH<sub>4</sub> and N<sub>2</sub>O dynamics in the boreal forest–mire ecotone, *Biogeosciences*, 12, 281–297, <https://doi.org/10.5194/bg-12-281-2015>, 2015.

Tupek, B., Ortiz, C. A., Hashimoto, S., Stendahl, J., Dahlgren, J., Karlton, E., and Lehtonen, A.: Underestimation of boreal soil carbon stocks by mathematical soil carbon models linked to soil nutrient status, *Biogeosciences*, 13, 4439–4459, <https://doi.org/10.5194/bg-13-4439-2016>, 2016.

Tupek, B., Lehtonen, A., Mäkipää, R., and Salovaara, P.: Soil and understory CO<sub>2</sub> respiration, CH<sub>4</sub>, and N<sub>2</sub>O fluxes, tree biomass and litter, and soil carbon stock after a long-term N fertilization of a Scots pine forest in Finland [Data set]. *Zenodo*. <https://doi.org/10.5281/zenodo.13952779>, 2024.

Tupek, B.: R script: Reduced microbial respiration sensitivity to soil moisture following long-term N fertilization enhances soil carbon retention in a boreal Scots pine forest. (Version 1). *Zenodo*. <https://doi.org/10.5281/zenodo.14101489>, 2024.

Ullah, M. R., Carrillo, Y., and Dijkstra, F. A.: Drought-induced and seasonal variation in carbon use efficiency is associated with fungi:bacteria ratio and enzyme production in a grassland ecosystem, *Soil Biology and Biochemistry*, 155, 108159, <https://doi.org/10.1016/j.soilbio.2021.108159>, 2021.

Uri, V., Kukumägi, M., Aosaar, J., Varik, M., Becker, H., Aun, K., Löhmus, K., Soosaar, K., Astover, A., Uri, M., et al.: The dynamics of the carbon storage and fluxes in Scots pine (*Pinus sylvestris*) chronosequence, *Science of the Total Environment*, 817, 152973, <https://doi.org/10.1016/j.scitotenv.2022.152973>, 2022.

Wang, Y., and Liu, Q.: Comparison of Akaike information criterion (AIC) and Bayesian information criterion (BIC) in selection of stock–recruitment relationships, *Fisheries Research*, 77, 220–225, <https://doi.org/10.1016/j.fishres.2005.08.011>, 2006.

Wei, H., Chen, X., He, J., Zhang, J., and Shen, W.: Exogenous Nitrogen Addition Reduced the Temperature Sensitivity of Microbial Respiration without Altering the Microbial Community Composition, *Frontiers in Microbiology*, 8, <https://doi.org/10.3389/fmicb.2017.02382>, 2017.

Wu, J., Zhang, H., Cheng, X., and Liu, G.: Nitrogen addition stimulates litter decomposition rate: From the perspective of the combined effect of soil environment and litter quality, *Soil Biology and Biochemistry*, 179, 108992, <https://doi.org/10.1016/j.soilbio.2023.108992>, 2023.

Zhang, H., Goll, D. S., Manzoni, S., Ciais, P., Guenet, B., and Huang, Y.: Modeling the effects of litter stoichiometry and soil mineral N availability on soil organic matter formation using CENTURY-CUE (v1.0), Geoscientific Model Development, 11, 4779–4796, <https://doi.org/10.5194/gmd-11-4779-2018>, 2018.

Zhang, X., Guan, D., Li, W., Sun, D., Jin, C., Yuan, F., Wang, A., and Wu, J.: The effects of forest thinning on soil carbon stocks and dynamics: A meta-analysis, Forest Ecology and Management, 429, 36–43, <https://doi.org/10.1016/j.foreco.2018.06.027>, 2018.

Zhao, J.: FluxCalR: a R package for calculating CO<sub>2</sub> and CH<sub>4</sub> fluxes from static chambers, Journal of Open Source Software, 4, 1751, <https://doi.org/10.21105/joss.01751>, 2019.

## 695 Acknowledgements

The study was conducted in the HoliSoils project (Holistic management practices, modelling and monitoring for European forest soils) funded by the European Union's Horizon 2020 research and innovation program (Grant Agreement No. 101000289). This study has been done with affiliation to the UNITE Flagship funded by the Research Council of Finland (decision 357909). We thank our field team lead by Petri Salovaara for collecting high-quality measurements. We also thank  
700 Mikko Kukkola and Hannu Ilvesniemi for the tree biomass monitoring data. We used BioRender for designing the graphical abstract. We appreciate constructive comments of Marleen Pallandt and the referees.

## Data and code availability

Complete data set on GHG fluxes, soil temperature and moisture, tree biomass and litter production, and soil carbon stocks are archived and available on ZENODO (<https://doi.org/10.5281/zenodo.13889762>). The R scripts supporting results  
705 replication is also openly available on ZENODO (<https://doi.org/10.5281/zenodo.14101488>).

## Author contribution

BT, AL, RM designed the hypothesis and experimental design. RM and AL arranged research funding and oversaw project management. BT contributed to data collection and carried out the analysis. BT prepared the manuscript with contributions from all co-authors.

## 710 Competing interests

~~We have no competing interests.~~ Some authors are members of the editorial board of journal Biogeosciences.